

A FRACTURE MECHANICS APPROACH TO FATIGUE IN FLAKE GRAPHITE CAST IRON

R. N. Castillo and T. J. Baker

Department of Metallurgy & Materials Science, Imperial College, Prince Consort Road, London SW7 2BP, England

ABSTRACT

Fatigue tests have been carried out on a variety of flake graphite cast irons using both smooth bar specimens and pre-cracked fracture mechanics test pieces. The fatigue limit is found to be dominated by the graphite eutectic cell size and is relatively insensitive to the microstructure of the matrix. It is shown that the fatigue limit is defined by the threshold stress intensity for propagation, the initiating defect being determined by the eutectic cell size.

KEYWORDS

Cast iron; flake graphite; fatigue; threshold; short cracks.

INTRODUCTION

At first sight, the fatigue behaviour of flake graphite cast iron would appear to be similar to that of steel. For example, smooth bar tests on cast iron reveal a pronounced "knee" in the load endurance curve leading to a fatigue limit. Also, as with many metals, the ratio of fatigue limit to tensile strength (i.e. the endurance ratio) is typically about 0.4 for a pearlitic cast iron. In view of these similarities, design procedures for flake graphite cast iron tend to follow those for initiation-dominated fatigue in other metallic materials although safety factors tend to be rather more generous. Closer inspection of the behaviour of flake graphite irons, however, reveals a number of important differences from conventional metals. First, there is a major difference in the nature of the tensile strength; whereas in most metals this is a measure of the stress for post-yield tensile instability, in flake graphite cast iron the tensile strength is typically about 30% of the yield strength (measured in compression) (Mitchell, 1977) and is in fact a brittle fracture stress which is determined by the fracture toughness of the iron and the size of the graphite flakes which act as cracklike defects (Venkatasubramanian and Baker, 1978). Consequently, if the endurance ratio is considered in terms of yield strength rather than tensile strength, it becomes apparent that

flake graphite irons have anomalously low fatigue resistance. A second major difference is that whereas in most metals the smooth-bar fatigue strength can be increased by hardening the material by alloying or heat treatment this is not so for flake graphite cast iron. For example, whilst large increases in the hardness of cast iron can be achieved by quenching from the austenite followed by tempering, this is not accompanied by any significant improvement in fatigue strength (Eagan, 1948; Mitchell, 1977). By comparison, surface hardening treatments which result in the development of residual surface compressive stresses are effective in increasing the fatigue strength in bending. A third unusual feature of flake irons is that when compared to steels of comparable hardness, they are remarkably insensitive to the presence of small surface notches. For notches of large geometry the notch sensitivity approaches that of steel (Angus, 1976). All of the above observations can be reconciled if fatigue in cast iron is a propagation-controlled process in which the graphite flakes act as pre-existing crack-like flaws.

MATERIAL

To produce samples of cast iron having different graphite flake sizes and hence different tensile strengths, a cupola-melted iron having a carbon equivalent value of 4.1, was cast in a sand mould to produce stepped test bars having section thicknesses of 12.5 mm and 50 mm. In both section thicknesses, the graphite was present as randomly dispersed type "A" graphite. The eutectic cell size was determined and, as shown in Table 1, there was about a factor of 3 difference in the scale of the graphite in the two section thicknesses.

TABLE 1. Fatigue Results From Flake Graphite Cast Iron

Matrix micro-structure	Eutectic cell size mm	Tensile strength MPa	Fatigue load ratio R	Fatigue limit (σ_{max}) MPa	crack growth parameters			
					C $\times 10^{12}$	m	ΔK_{TH} $MNm^{-3/2}$	ΔK_{TH} from fatigue limit $MNm^{-3/2}$
Pearlite	0.49	294	0.1	112	4.1	6.6	9.2	3.6
Pearlite	1.51	253	0.1	78	0.7	7.0	10.9	4.4
Tempered martensite	1.51	404	0.1	72	6.7	6.4	7.4	4.1
Ferrite	1.51	160	0.1	60	4.9	6.6	7.0	3.4
Pearlite	1.51	253	0.3	-	2.6	7.4	6.9	-

In the as-cast condition, the matrix microstructure was wholly pearlitic. For the 50 mm thick section, different matrix microstructures were produced by heat treatment. A completely ferritic matrix was produced by slow cooling from the austenite. A tempered martensitic matrix was produced by oil quenching from the austenite followed by tempering at 500 °C.

TESTING PROCEDURES

Fatigue testing utilised both smooth and pre-cracked test pieces. In both cases, tension test geometries were employed. Testing of the smooth bar specimens was carried out under conditions of constant amplitude loading with a constant R-ratio of 0.1. Compact tension fracture mechanics specimens were employed for crack propagation measurements. The specimen thickness readily satisfied the requirements for plane strain condition studied, crack growth data was obtained under conditions of both decreasing and increasing alternating stress intensity. Crack growth was monitored by a D.C. potential drop technique. Growth rates were measured down to 10^{-7} mm/cycle and the value of the alternating stress intensity corresponding to this growth rate is referred to here as the threshold alternating stress intensity ΔK_{TH} . Most of the crack propagation tests were performed at an R-ratio of 0.1. However, for the 50 mm section thickness in the as-cast condition, a series of tests was also undertaken at an R-ratio of 0.3.

RESULTS

The results of the smooth-bar fatigue tests are summarised in Table 1. Considering first the two as-cast conditions in which the matrix microstructure was fully pearlitic, it will be seen that refinement of the graphite flake structure is accompanied by a substantial increase in fatigue strength. By comparison, when the flake geometry is held constant and the matrix is hardened by heat treatment, it is found that the fatigue limit decreases despite a substantial improvement in tensile strength. With the ferritic matrix, there is a reduction in both fatigue limit and tensile strength. These observations are in accord with those made by earlier workers (Eagan, 1948).

The results of the crack propagation studies are illustrated in Figs 1 and 2 and summarised in Table 1. For all of the conditions examined, the crack growth behaviour at higher values of ΔK obeys the Paris relationship:

$$da/dN = C\Delta K^m.$$

At low values of ΔK , an apparent threshold condition is attained. The value of the exponent m in the growth rate equation was about 7 for all of the conditions tested. This is much higher than the values usually observed for metallic materials which are between 3 and 4. The unusually high ΔK dependence suggests that the fatigue crack is not propagating by a simple ductile striation mechanism but involves a substantial contribution from brittle monotonic modes of fracture (Ritchie and Knott, 1973). The latter is also indicated by the strong load ratio dependence which is illustrated in Fig. 1.

Considering now the influence of the microstructural variables, Fig. 1 indicates that for the as-cast condition a refinement in the graphite flake geometry produces a small increase in growth rate and a reduction in the fatigue threshold. For both conditions, the threshold values are substantially higher than those normally observed in steels. This is often the case when unusually high m -values are encountered and has been attributed to an increased crack closure effect arising from the increased surface roughness associated with the presence of monotonic fracture processes (Mayes and Baker, 1981). In flake graphite cast irons, the fatigue fracture surfaces are much more irregular than in conventional

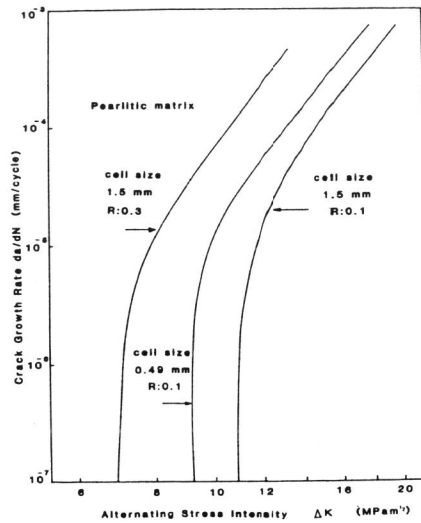


FIG. 1. Effect of cell size and R-ratio on fatigue crack propagation of pearlitic iron

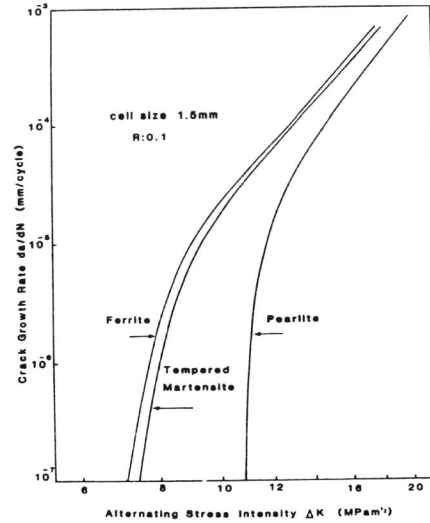


FIG. 2. Effect of matrix microstructure on crack propagation behaviour of cast iron

metallic materials and usually it is not possible to distinguish between fatigue and fast fracture. The K_{TH} value was lower for the cast iron having the finer flake size and this was reflected in a visibly smoother fracture surface.

The heat-treated irons having ferrite and tempered martensite matrix microstructures exhibit nearly identical crack propagation behaviour, Fig. 2. Crack growth rates are higher than in the as-cast pearlitic condition but the major difference is that the fatigue threshold values are much lower and more typical of values associated with steel. It is also of note that the fatigue fracture surfaces for the heat-treated irons appeared much smoother than those obtained from the as-cast structures.

FRACTOGRAPHY

Figure 3 shows a section through a fatigue crack in an as-cast pearlitic iron. It can be seen that the crack has initiated at the smooth surface from a favourably oriented graphite flake. The subsequent propagation of the crack has then proceeded preferentially via suitably oriented flakes. Further insight into the mechanism of crack propagation is provided by examination of the fracture surfaces in the scanning electron microscope. As shown in Fig. 4 the fracture surface is extremely rough with a substantial proportion of the surface being occupied by graphite flakes. Eutectic cells can be distinguished and it is of note that the graphite flakes are continuous across the eutectic cell. This suggests that the relevant microstructural dimension of the graphite as far as fracture is concerned is the eutectic cell diameter rather than the flake size as revealed on polished sections. In the case of irons having pearlitic or martensitic microstructures it is extremely difficult to identify individual fatigue



FIG. 3. Fatigue crack developing from smooth surface in flake graphite cast iron

striations as the crack traverses the matrix. In the ferritic iron, striations could occasionally be distinguished and their geometry indicated that they radiated from individual graphite flakes. This suggests that the graphite facilitates fatigue crack propagation in two ways; first it fractures in a brittle manner by interface decohesion or basal plane cleavage, secondly the resultant internal crack can act as a secondary site for fatigue crack development.

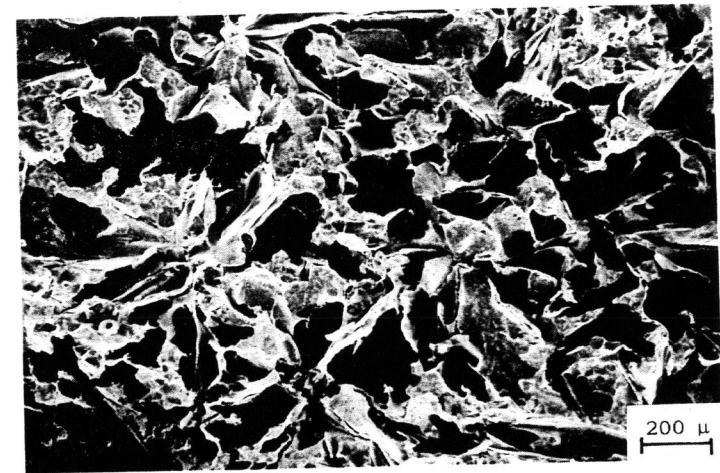


FIG. 4. Fatigue fracture surface from flake graphite cast iron

DISCUSSION

The observed effects of microstructural variables on the smooth bar fatigue behaviour and the fractographic evidence indicate that fatigue in nominally smooth samples of flake graphite cast iron is a propagation-controlled process in which the graphite flakes act as pre-existing crack-like defects. Thus a change in the dimensions of the graphite flakes has a pronounced effect on the fatigue strength whereas large changes in the microstructure and properties of the steel-like matrix produce small changes in the fatigue limit due to their relatively small influence on the crack propagation behaviour. It follows that from a knowledge of the crack propagation behaviour and the flake geometry it should be possible to predict the fatigue behaviour of nominally smooth bar samples. Detailed analysis of this problem is complicated by the fact that the graphite flakes are numerous, randomly oriented and their separation is small in relation to their length. Consequently there will inevitably be interactions between the stress fields associated with adjacent flakes. Nevertheless, as a first approximation one can consider a single surface-breaking graphite cell as a pre-existing short crack. The stress intensity factor for a semi-circular edge crack of depth a is given by

$$K = 0.7 \sigma \sqrt{\pi a} \quad (1)$$

If the smooth bar fatigue limit corresponds to the attainment of the threshold alternating stress intensity ΔK_{TH} at a graphite-nucleated short crack

$$\Delta K_{TH} = 0.7 \sigma_{max} (1-R) \sqrt{\pi a} \quad (2)$$

where σ_{max} is the maximum stress at the fatigue limit for the specified R-ratio. As discussed above, the relevant graphite flake size as far as fracture processes in cast iron are concerned is the diameter of the eutectic cell. The values quoted in Table 1 refer to mean cell diameters as measured on metallographically prepared plane sections. To obtain the corresponding volumetric diameters, these values have to be multiplied by a factor of $\sqrt{2}$. Short crack ΔK_{TH} values obtained by inserting the relevant smooth bar data in equation 2 are shown in Table 1 together with the values measured from the long crack fracture mechanics specimens. It is of note that the short crack values are substantially smaller. The other interesting observation is that the short crack ΔK_{TH} values are very similar for all of the microstructural conditions examined.

Similar differences between long and short crack ΔK_{TH} values to those shown here have been reported by others; for example, in a recent study of a nickel-base superalloy, McCarver and Ritchie (1982) found that the short crack threshold was approximately 60% of the long crack value. Such differences in threshold values may be attributed to the crack closure phenomenon. When thresholds are determined using fracture mechanics specimens containing large preceeding fatigue cracks, the inherent roughness of the fracture surfaces prevents the crack from closing completely during the unloading part of the cycle. This wedging action at the crack tip reduces the effective alternating stress intensity to which the material is exposed. It follows that the apparent threshold value measured under such conditions will be greater than the true value experienced by the crack tip. In the case of the pre-existing short crack, there is no preceeding fracture surface and hence nothing to prevent complete closure of the crack faces. Under these conditions the measured ΔK_{TH} is expected to be more

representative of the true value for the material. The magnitude of the closure effect and hence the difference between long and short crack thresholds depends on the roughness of the fatigue fracture surface. As noted above, fatigue fractures in flake graphite cast iron are extremely rough as compared to those in wrought steel and hence a large difference between short and long crack thresholds is to be expected.

In view of the preceeding observations regarding the effects of crack closure, it is suggested that the ΔK_{TH} values calculated from the fatigue limit data are a more reliable indication of the true fatigue threshold for flake graphite cast iron than values obtained from the fracture mechanics specimens. Support for this proposition is provided by the observation that when ΔK_{TH} values for steels are determined under conditions of minimal closure, for example under conditions of high R-ratio, similar values of between 3 and 5 $\text{MNm}^{-3/2}$ are obtained (Fuchs, 1980). Also, as in the case of the cast iron samples, it is found that these true threshold values are insensitive to the microstructure of the steel.

It is concluded that the fatigue behaviour of nominally defect-free samples of flake graphite cast iron can be adequately explained in terms of a crack propagation model in which the graphite eutectic cells act as pre-existing short cracks.

CONCLUSIONS

1. The smooth bar fatigue strength of flake graphite cast iron is sensitive to the size of the graphite eutectic cell, finer cell size giving higher fatigue strength.
2. Modification of the matrix microstructure by heat treatment has little effect on the fatigue limit despite producing substantial changes in tensile strength.
3. The exponent relating crack growth rate to ΔK is much higher than in most metallic materials due to the extensive participation of graphite flakes in the fatigue crack propagation process.
4. ΔK_{TH} values obtained from fracture mechanics specimens vary from 7 to 11 $\text{MNm}^{-3/2}$ for the microstructural conditions tested. It is proposed that crack closure effects arising from the very rough nature of the fatigue fracture surface are responsible for the ΔK_{TH} values being higher than those usually observed in steel.
5. Short crack ΔK_{TH} values calculated from the nominally smooth bar fatigue tests are substantially lower than the long crack thresholds and are relatively insensitive to the microstructural condition of the cast iron matrix.
6. The reduced ΔK_{TH} values obtained from the graphite-nucleated smooth bar tests are attributed to the absence of crack closure effects.
7. The fatigue limit is determined by a threshold stress intensity for crack propagation, the initiating short crack being determined by the eutectic cell size.

ACKNOWLEDGEMENTS

The authors would like to thank the British Cast Iron Research Association for supplying the experimental materials and Professor D W Pashley for the provision of research facilities at Imperial College. One of us (RNC) would also like to thank the World University Service for financial support.

REFERENCES

- Angus, H. T. (1976). Cast iron: physical and engineering properties. Butterworths, London.
- Eagen, T. E. (1948). Trans. Amer. Foundrymen's Soc., 64, 230.
- Fuchs, H. O. and Stephens, R. I. (1980). Metals fatigue in engineering. Wiley Interscience Publications, New York. p.301.
- Mayes, I. C. and Baker, T. J. (1981). J. Fatigue of Eng. Mater. and Struct., 4, 135.
- McCarver, J. F. and Ritchie, R. O. (1982). J. Mater. Sci. Eng., 55, 63.
- Mitchell, M. R. (1977). A.F.S. Int. Cast Metals Journal, 2, 64.
- Ritchie, R. O. and Knott, J. F. (1973). Acta Met., 23, 639.
- Venkatasubramanian, T. V. and Baker, T. J. (1978). Metals Technology, 5, 57.